AIAA JOURNAL
Vol. 30, No. 12, December 1992

Effects of Interply Damping Layers on the Dynamic Characteristics of Composite Plates

D. A. Saravanos* and J. M. Pereira†
NASA Lewis Research Center, Cleveland, Ohio 44135

Integrated damping mechanics for composite plates with constrained interlaminar layers of polymer damping materials are developed. Discrete layer damping mechanics are presented for composite laminates with damping layers, in connection with a semianalytical method for predicting the modal damping in simply supported specialty composite plates. Correlations between predicted and measured response in graphite/epoxy plates illustrate the accuracy of the method. Additional application cases for graphite/epoxy plates of various laminations demonstrate the potential for higher damping than geometrically equivalent aluminum plates. The effects of aspect ratio, damping layer thickness, and fiber volume ratio on static and dynamic characteristics of the composite plate are also investigated.

Introduction

DAMPING is a significant dynamic parameter for vibration and sound control, dynamic stability, positioning accuracy, fatigue endurance, and impact resistance. Many current structural applications (e.g., large space structures, engine blades, and high-speed machinery) require light weight and high dynamic performance. Therefore, candidate sources of passive damping should add minimal parasitic weight and be compatible with the structural configuration.

Two potential damping sources satisfying the previous requirements are the constrained damping layer approach and the damping capacity of composites. Constrained damping layers in isotropic metallic structures have been widely applied and investigated.[1] They provide high damping, but tend to increase the structural weight and offer limited means for damping tailoring. The inherent damping capacity of composite materials also seems promising. Although the damping of composite structures is not very high, it is significantly higher than that for most common metallic structures. Moreover, composites are the materials of preference in many cases, since they readily provide high specific stiffness and strength. More importantly, research on the damping mechanics of composite laminates[2-4] and structures[5,6] has shown that composite damping is anisotropic, highly tailorable, and depends on an array of micromechanical, laminate, and structural parameters. It has been further demonstrated that optimal tailoring may significantly improve the damped dynamic performance of composite structures.[7]

It seems likely that the combination of both approaches (i.e., composite structures with interlaminar damping layers) will offer the advantages of high damping, damping tailoring, good mechanical properties, and low weight addition. In addition, the interlaminar damping concept is highly compatible with the laminated configuration of composite structures and their fabrication techniques. In contrast to isotropic materials, the variations in anisotropy and elastic properties of each composite ply typically induce high interlaminar stresses; hence, interlaminar layers may produce higher and also tailorable damping. However, other critical mechanical properties, such as stiffness and strength, are expected to be reduced. In view of the complexity of the problem, it is very desirable to develop integrated composite mechanics that will efficiently predict the damping of composite structures with interlaminar damping layers, together with other critical mechanical properties and dynamic characteristics. Limited analytical and experimental work has been reported in this direction, including the damping of specialty composite truss members and plates[8-11] and the damping analysis of simple composite beams using continuum finite element simulations.[12,13]

This paper presents recent developments in integrated damping mechanics for composite laminates with interlaminar damping layers. The laminate mechanics are general in that they incorporate the capability for arbitrary numbers of plies and damping layers, arbitrary fiber orientations, and arbitrary fiber volume ratios (FVRs). They also include the capacity to simulate the damping of extensional, bending, and coupled deformations. The theory assumes a general piecewise continuous displacement field through the thickness of the laminate. The damping mechanics for composite laminates with damping layers is also integrated with other composite mechanics theories[14,15] in order to include the effects of the many composite parameters on the dynamic characteristics. Finally, a semianalytical methodology for the prediction of the dynamic properties of simply supported (SS) specialty thick composite plates with interlaminar damping layers is developed.

To validate the methodology, measured and predicted frequency response functions of T300/934 graphite/epoxy plates with damping layers are compared. Predicted modal damping values, natural frequencies, and static deflections of additional graphite/epoxy composite plates are presented. The effects of various cross-ply configurations, aspect ratio, damping layer thickness, and FVR on the damped dynamic characteristics are also investigated.

Methodology

This section first reviews the synthesis of the composite properties for each composite ply and interlaminar layer. Then the developed damping mechanics for composite laminates with interply layers (Fig 1a) and the dynamic analysis of specialty composite plates with interlaminar damping layers are presented.

Composite Properties

For a unidirectional composite loaded along the material axes, closed-form expressions have been developed for the

Presented as Paper 91-1124 at the AIAA/ASME/ASCE/AHS/ASC 32nd Structures, Structural Dynamics, and Materials Conference, Baltimore, MD, April 8-10, 1991; received Oct. 18, 1991; revision received May 13, 1992; accepted for publication May 13, 1992.

*Resident Research Associate, 21000 Brookpark, MS 49-8. Member AIAA.
†Aerospace Engineer, 21000 Brookpark, MS 49-8.

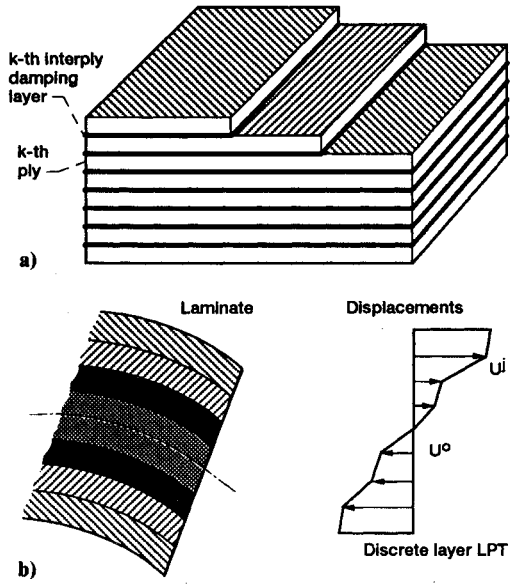

Fig. 1 Laminates with interlaminar damping layers: a) typical laminate configuration; b) kinematic assumptions of discrete-layer laminate theory.

synthesis of elastic and dissipative properties.[14,15] Five independent elastic parameters completely characterize the stiffness of a unidirectional composite (orthotropic but transversely isotropic material): 1) the in-plane longitudinal modulus E_{l11}, 2) the transverse in-plane modulus E_{l22}, 3) the in-plane Poisson's ratio ν_{l12}, 4) the in-plane shear modulus G_{l12}, and 5) the interlaminar shear modulus G_{l23}. Additionally, four independent damping loss factors characterize the composite damping: the longitudinal loss factor η_{l1} (direction 11), the transverse in-plane damping η_{l2} (direction 22), the transverse through-the-thickness damping $\eta_{l3} = \eta_{l2}$ (direction 33), the in-plane shear damping η_{l6} (direction 12), the interlaminar shear damping η_{l4} (direction 23), and the interlaminar shear damping $\eta_{l5} = \eta_{l6}$ (direction 13). Both damping and elastic properties are explicitly related to fiber/matrix properties[14] and the FVR.

The interlaminar layers are assumed isotropic. Two independent elastic properties (Young's modulus and Poisson's ratio) and two independent damping properties (normal and shear loss factors) completely characterize their viscoelastic behavior at a given frequency and temperature.

Off-Axis Composites

For the case of off-axis composites (i.e., composites loaded at an angle θ), the following transformations provide the stiffness matrix $[E_c]$ and the damping matrix $[\eta_c]$, respectively[14,15]:

$$[E_c] = [R]^{-1}[E_l][R]^{-T} \tag{1}$$

$$[\eta_c] = [R]^{T}[\eta_l][R]^{-T} \tag{2}$$

where $[E_l]$ is the stiffness matrix of the composite in the material coordinate system, and $[\eta_l]$ represents the on-axis composite damping. The transformation matrix $[R]$ and the damping matrices $[\eta_l]$ and $[\eta_c]$ are shown in the Appendix.

For the interlaminar layers that are assumed isotropic, Eqs. (1) and (2) are reduced to trivial cases. In this manner, and contrary to many reported studies involving simplifying assumptions, all independent elastic and dissipative properties of the composite plies and the interlaminar laminas are considered.

Laminates with Interlaminar Damping Layers

To model the damping of laminates with interlaminar damping layers, a discrete layer laminate damping theory (DLDT) incorporating a piecewise continuous displacement field through the thickness is developed. Compared to other laminate theories based on assumed continuous displacement fields, the DLDT provides the capacity for more accurate strain and dissipative energy calculations in each ply, particularly in each damping layer. The kinematic assumptions for the laminate theory are schematically shown in Fig. 1b. Discrete layer theories were originally proposed by Grigolyuk and were subsequently generalized by other researchers (see Refs. 16 and 17) for the more accurate calculation of stresses in thick laminates. However, with additional development presented here, the DLDT combines the potential for accurate damping predictions in composite laminates with damping layers, while maintaining generality and elegance. The assumed displacement field has the following form:

$$\begin{aligned} u(x, y, z, t) &= u^0(x, y, t) + \bar{u}(x, y, z, t) \\ v(x, y, z, t) &= v^0(x, y, t) + \bar{v}(x, y, z, t) \\ w(x, y, z, t) &= w^0(x, y, t) \end{aligned} \tag{3}$$

where superscript 0 represents the uniform through-the-thickness midplane deflection. Assuming that the displacements are separable functions of z, as suggested by Reddy and co-workers,[17] Eqs. (3) take the following form:

$$\begin{aligned} u(x, y, z, t) &= u^0(x, y, t) + \sum_{j=1}^{N} u^j(x, y, t)F^j(z) \\ v(x, y, z, t) &= v^0(x, y, t) + \sum_{j=1}^{N} v^j(x, y, t)F^j(z) \\ w(x, y, z, t) &= w^0(x, y, t) \end{aligned} \tag{4}$$

where u^j and v^j are displacements along the x and y directions, respectively, preferably at the interfaces between composite plies or sublaminates (group of plies) and the interlaminar damping layers. $F^j(z)$ are interpolation functions. In this manner the assumed in-plane displacement field is general, in that it may represent extensional, flexural, shear, and coupled deformations, as well as the interlaminar shear strains through the thickness of the laminate.

The laminate strains are directly derived from Eqs. (4):

$$\begin{aligned} \epsilon_{ci} &= \epsilon^0_{ci} + \sum_{j=1}^{N} \epsilon^j_{ci}F^j(z), \qquad i = 1, 2, 6 \\ \epsilon_{ci} &= \epsilon^0_{ci} + \sum_{j=1}^{N} \epsilon^j_{ci}F^j_{,z}(z), \qquad i = 4, 5 \end{aligned} \tag{5}$$

where the midplane strains are

$$\begin{aligned} &\epsilon^0_{c1} = u^0_{,x}, \qquad \epsilon^0_{c2} = v^0_{,y}, \qquad \epsilon^0_{c6} = u^0_{,y} + v^0_{,x} \\ &\epsilon^0_{c4} = w^0_{,y}, \qquad \epsilon^0_{c5} = w^0_{,x} \end{aligned} \tag{6}$$

and the generalized strains are

$$\begin{aligned} &\epsilon^j_{c1} = u^j_{,x}, \qquad \epsilon^j_{c2} = v^j_{,y}, \qquad \epsilon^j_{c6} = u^j_{,y} + v^j_{,x} \\ &\epsilon^j_{c4} = v^j, \qquad \epsilon^j_{c5} = u^j \end{aligned} \tag{7}$$

The comma in the subscripts indicates differentiation.

The dissipated strain energy per unit area of the laminate, Δw_L, is

$$\Delta w_L = \frac{1}{2}\int_{-h/2}^{h/2} 2\pi\epsilon_c^T[E_c]\,[\eta_c]\epsilon_c\,dz \tag{8}$$

Combination of Eqs. (8) and (5-7) ultimately provides the dissipated strain energy per unit area:

$$\Delta w_L = \frac{1}{2}\left(\epsilon_c^{0T}[A_d]\epsilon_c^0 + 2\epsilon_c^{0T}\sum_{j=1}^{N}[B_d^j]\epsilon_c^j + \sum_{j=1}^{N}\sum_{m=1}^{N}\epsilon_c^{jT}[D_d^{jm}]\epsilon_c^m\right) \tag{9}$$

where $[A_d]$ is the extensional laminate damping matrix, including out-of-plane shear terms. The generalized coupling damping matrices $[B_d^j]$ and flexural/shear matrices $[D_d^{jm}]$ are new. The matrix expressions in Eq. (9) are given by

$$[A_d] = 2\pi\sum_{k=1}^{N_l}\int_{h_{k-1}}^{h_k}[E_c]_k[\eta_c]_k\,dz$$

$$(B_d^j)_{in} = 2\pi\sum_{k=1}^{N_l}\int_{h_{k-1}}^{h_k}([E_c]_k[\eta_c]_k)_{in}F^j(z)\,dz, \qquad i, n = 1, 2, 6$$

$$(B_d^j)_{in} = 2\pi\sum_{k=1}^{N_l}\int_{h_{k-1}}^{h_k}([E_c]_k[\eta_c]_k)_{in}F^j_{,z}(z)\,dz, \qquad i, n = 4, 5 \tag{10}$$

$$(D_d^{jm})_{in} = 2\pi\sum_{k=1}^{N_l}\int_{h_{k-1}}^{h_k}([E_c]_k[\eta_c]_k)_{in}F^j(z)F^m(z)\,dz \qquad i, n = 1, 2, 6$$

$$(D_d^{jm})_{in} = 2\pi\sum_{k=1}^{N_l}\int_{h_{k-1}}^{h_k}([E_c]_k[\eta_c]_k)_{in}F^j_{,z}(z)F^m_{,z}(z)\,dz \qquad i, n = 4, 5$$

where N_l is the number of composite plies and damping layers. The maximum laminate strain energy per unit area, w_L, is, by definition,

$$w_L = \frac{1}{2}\int_{-h/2}^{h/2}\epsilon_c^T[E_c]\epsilon_c\,dz \tag{11}$$

Combination of Eqs. (11) and (5-7) provides the maximum strain energy as a separable form of material properties and strains:

$$w_L = \frac{1}{2}\left(\epsilon_c^{0T}[A]\epsilon_c^0 + 2\epsilon_c^{0T}\sum_{j=1}^{N}[B^j]\epsilon_c^j + \sum_{j=1}^{N}\sum_{m=1}^{N}\epsilon_c^{jT}[D^{jm}]\epsilon_c^m\right) \tag{12}$$

where $[A]$ is the extensional laminate stiffness matrix with additional out-of-plane shear terms, $[B^j]$ are the generalized coupling stiffness matrices, and $[D^{jm}]$ are the flexural/shear matrices given by

$$[A] = \sum_{k=1}^{N_l}\int_{h_{k-1}}^{h_k}[E_c]_k\,dz$$

$$(B^j)_{in} = \sum_{k=1}^{N_l}\int_{h_{k-1}}^{h_k}([E_c]_k)_{in}F^j(z)\,dz, \qquad i, n = 1, 2, 6$$

$$(B^j)_{in} = \sum_{k=1}^{N_l}\int_{h_{k-1}}^{h_k}([E_c]_k)_{in}F^j_{,z}(z)\,dz, \qquad i, n = 4, 5 \tag{13}$$

$$(D^{jm})_{in} = \sum_{k=1}^{N_l}\int_{h_{k-1}}^{h_k}([E_c]_k)_{in}F^j(z)F^m(z)\,dz, \qquad i, n = 1, 2, 6$$

$$(D^{jm})_{in} = \sum_{k=1}^{N_l}\int_{h_{k-1}}^{h_k}([E_c]_k)_{in}F^j_{,z}(z)F^m_{,z}(z)\,dz, \qquad i, n = 4, 5$$

The equivalent laminate loss factor for a given local displacement field is

$$\eta_L = \Delta w_L/(2\pi w_L) \tag{14}$$

In both Eqs. (10) and (13), the interlaminar damping layers are considered as individual plies having isotropic elastic and damping matrices $[E_c]$ and $[\eta_c]$, respectively. For a given interlaminar layer, $[\eta_c]$ is determined from the mechanical properties of the material as a trivial composite case (Ref. 14). In this manner the proposed laminate damping mechanics are general, since they can handle any number of composite plies, damping layers, and laminate configurations.

Simply Supported Composite Plates

The damped dynamic characteristics of simply supported specialty composite plates with interlaminar damping layers are calculated based on the previously described discrete-layer laminate damping theory. As will be shown in the remaining section, in the special case of composite plates consisting of 0- and 90-deg plies, exact semianalytical modal analysis solutions exist. Hence, exact and computationally inexpensive predictions of static and dynamic characteristics (modal damping and natural frequencies) are possible that will provide valuable insight in the mechanics of the problem and will establish the critical parameters. Most other laminations, boundary conditions, and structural configurations require approximate solutions; these methods will be presented in the near future.

Assuming a rectangular α by β symmetric simply supported (SS) composite plate with negligible coupling ($A_{16} = A_{26} = 0$, $B_{16}^j = B_{26}^j = 0$, $D_{16}^{jm} = D_{26}^{jm} = 0$), the following Navier fundamental solutions form a complete set of mode shapes in the x-y plane:

$$\begin{aligned}
u_{mn}^0(x, y, t) &= U_{mn}^0\cos(ax)\sin(by)e^{i\omega t}\\
v_{mn}^0(x, y, t) &= V_{mn}^0\sin(ax)\cos(by)e^{i\omega t}\\
w_{mn}^0(x, y, t) &= W_{mn}^0\sin(ax)\sin(by)e^{i\omega t}\\
u_{mn}^j(x, y, t) &= U_{mn}^j\cos(ax)\sin(by)e^{i\omega t}\\
v_{mn}^j(x, y, t) &= V_{mn}^j\sin(ax)\cos(by)e^{i\omega t}
\end{aligned} \tag{15}$$

Where $a = m\pi/\alpha$ and $b = n\pi/\beta$. The fundamental solutions in Eqs. (15) are consistent with the boundary conditions of the plate:

$$\begin{aligned}
w_{mn}^0 = u_{mn}^0 = u_{mn}^j = N_y^0 = N_y^j = 0 \qquad &\text{at} \qquad y = 0, \beta\\
w_{mn}^0 = v_{mn}^0 = v_{mn}^j = N_x^0 = N_x^j = 0 \qquad &\text{at} \qquad x = 0, \alpha
\end{aligned} \tag{16}$$

where N_x^0 and N_x^j are the resultant generalized forces in the x direction, and N_y^0 and N_y^j are the forces in the y direction.

Combination of Eqs. (6), (7), and (15) yields the modal midplane and generalized strains as separable functions of x, y coordinates, time, and amplitudes:

$$\{\epsilon^0\}_{mn} = [B_{mn}^0]\{U_{mn}^0\}e^{i\omega t}, \qquad \{\epsilon^j\}_{mn} = [B_{mn}^j]\{U_{mn}^j\}e^{i\omega t} \tag{17}$$

where the terms in matrices $[B_{mn}]$ are sine/cosine functions of x, y coordinates and mode order. The amplitude displacement vectors are $U^0 = \{U^0, V^0, W^0\}^T$ and $U^j = \{U^j, V^j\}^T$. The kinetic energy through the thickness of the plate is

$$K_L = \frac{1}{2}\int_{-h/2}^{h/2}\{\dot{u}\}^T\rho\{\dot{u}\}\,dz \tag{18}$$

Considering Eqs. (4), the laminate kinetic energy per unit area takes the following form:

$$K_L = \frac{1}{2}\left(\{\dot{u}^0\}^T[A_M]\{\dot{u}^0\} + 2\{\dot{u}^0\}^T\sum_{j=1}^{N}[B_M^j]\{\dot{u}^j\} + \sum_{j=1}^{N}\sum_{m=1}^{N}\{\dot{u}^j\}^T[D_M^{jm}]\{\dot{u}^m\}\right) \tag{19}$$

where the generalized laminate mass and inertia matrices are

$$[A_M] = \sum_{k=1}^{N_l} \int_{h_{k-1}}^{h_k} \text{diag}(\rho_k)\, dz$$
$$[B_M^j] = \sum_{k=1}^{N_l} \int_{h_{k-1}}^{h_k} \text{diag}(\rho_k) F^j(z)\, dz \quad (20)$$
$$[D_M^{jm}] = \sum_{k=1}^{N_l} \int_{h_{k-1}}^{h_k} \text{diag}(\rho_k) F^j(z) F^m(z)\, dz$$

The term $\text{diag}(\rho_k)$ indicates a diagonal matrix, with all diagonal terms equal to the density of the kth ply. The kinetic energy in Eq. (19) includes the contributions of rotational inertia.

By substituting Eqs. (15) into the strain and kinetic energy expressions for the laminate, Eqs. (12) and (19), respectively, integrating over the plate area, and applying Lagrangian dynamics, it can be proved that the undamped modal analysis (free vibration) solution of the plate takes the following form:

$$-\omega_{mn}^2 [M_{mn}] U_{mn} + [K_{mn}] U_{mn} = 0 \quad (21)$$

where the through-the-thickness modal displacements are $\{U_{mn}\} = \{U_{0mn}; U_{1mn}, \ldots, U_{Nmn}\}$ and the subscripts m and n indicate the mode order. Numerical solution of this eigenvalue problem provides the natural frequencies ω_{mn} and the through-the-thickness modes $\{U_{mn}\}$ for each order mn of plane modes, in the context of Eqs. (15).

The modal damping associated with the mnth vibration mode η_{mn} is

$$\eta_{mn} = \frac{1}{2}\pi \left(\int_V \Delta w_{mn}\, dV \Big/ \int_V w_{mn}\, dV \right) \quad (22)$$

where Δw_n and w_n represent the dissipated and maximum specific modal strain energies per cycle, respectively. For laminated composite plates the modal damping becomes

$$\eta_{mn} = \frac{1}{2}\pi \left(\int_A \Delta w_{mn}\, dA \Big/ \int_A w_{Lmn}\, dA \right) \quad (23)$$

where Δw_{Lmn} and w_{Lmn} are, respectively, the dissipated and maximum laminate modal strain energies of the mnth mode. To calculate the modal damping, Eqs. (10) and (13) are integrated through the thickness, and are combined with Eqs. (9) and (12), respectively. Then the generalized stresses and strains are related to the calculated mode shape using Eqs. (15). The integrations over the area of the plate are performed analytically. Since the natural frequencies and the mode shapes through the thickness are calculated numerically from Eq. (20), the whole procedure is semianalytical.

Frequency Effects

Many properties of polymers are sensitive to frequency and environmental conditions. These effects are more predominant on the damping layer, since these polymers are typically near the glass transition. On the other hand, typical matrix polymers in the composite plies are less sensitive to frequency at normal temperatures, since they have much higher glass transition temperatures. The effects of frequency ω and temperature T on moduli E and damping η are approximated as follows:

$$E = E_0 + (E_g - E_0) f_1(\omega, T) \quad (24)$$

$$\eta = \eta_0 + (\eta_g - \eta_0) f_2(\omega, T) \quad (25)$$

where E and η represent both normal and shear properties, and the subscripts 0 and g indicate reference and glass transition conditions, respectively. The functions f_1 and f_2 interpolate the polymer behavior in the glassy range (from reference state to glass transition) and, if necessary, beyond the glass transition into the rubbery zone. Both functions are zero at reference conditions and unity at glass transition $T_g = T_g(\omega)$ and also depend on experimental data. In this context the moduli reach their maximum values at reference conditions and reduce to very low values at glass transition, whereas the damping loss factors peak at glass transition and are low in reference conditions.

Equations (24) and (25) readily approximate the frequency dependence of monolithic materials, as in the case of damping layers. The inclusion of frequency effects on the properties of composite plies may be accomplished through the micromechanics summarized in previous sections. The frequency effects propagate on the laminate stiffness and damping in the context of Eqs. (10) and (13). Finally, this results in frequency-dependent stiffness matrices $[K_{mn}]$ [Eq. (21)] and modal damping [Eq. (22)].

An iterative procedure was utilized for the solution of this nonlinear eigenvalue problem, that is, for each frequency the stiffness and damping matrices were updated, and the modal characteristics were recalculated until convergence was obtained for the specific mode. These frequency-dependent modal characteristics were used to synthesize the frequency response function when desirable. An alternative more accurate, but also computationally more elaborate, way to obtain the transfer functions would be the direct numerical solution of the dynamic system [Eq. (21)] with frequency-dependent stiffness and damping matrices.

Experimental Verification

To validate the accuracy of the method and experimentally verify the effects of damping layers on the dynamic response of composite plates, a composite plate with interlaminar damping was fabricated and tested (see Fig. 2). The plate was 11 in. × 11 in. (28 cm × 28 cm) and consisted of plies of 0.6 FVR T300/934 graphite/epoxy, combined with layers of ScotchDamp ISD110 damping film (3M Corp., St. Paul,

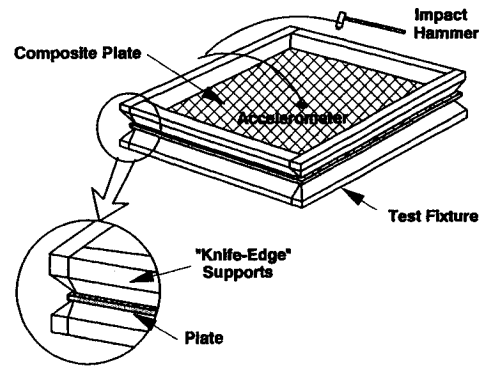

Fig. 2 Experimental configuration showing composite plate in knife-edge supports.

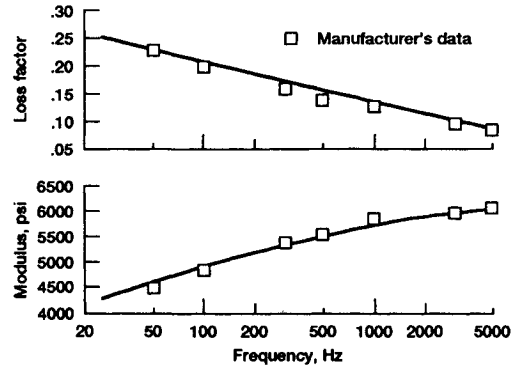

Fig. 3 Mechanical properties of the ISD110 damping polymer at 30°C: shear modulus and shear loss factor.

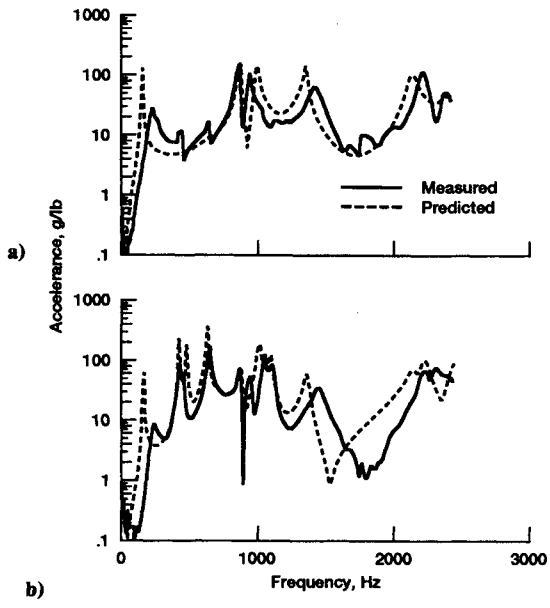

Fig. 4 Frequency response functions of a $(0_2/90_2/i/90_2/0_2)_s$ T300/934 plate with ISD110 damping layers: a) accelerance at center $(x/\alpha, y/\beta) = (1/2, 1/2)$; b) accelerance at point $(x/\alpha, y/\beta) = (1/4, 3/4)$.

MN), laid up in a $[0_2/90_2/i/90_2/0_2]_s$ configuration, where i denotes the damping layer. The shear loss factor and moduli of the damping polymer, as approximated by Eqs. (24) and (25), are shown in Fig. 3 for the frequency range of interest and represent average values of the polymer at 30°C provided in the manufacturer's data sheet. The nominal thicknesses of the graphite/epoxy tape and damping layers were 0.006 in. (0.15 mm) and 0.005 in. (0.13 mm), respectively. The plate was laid up by hand, co-cured at 350°F (175°C) and 50 psi (345 KPa), and finally cut to size.

Frequency response functions for the composite plate were obtained from impulse tests. A special fixture with "knife-edge" supports was designed (see Fig. 2) to support as closely as possible the plate in the SS configuration described by Eqs. (16) and to minimize the friction forces. The plate was impacted at the quarter point $(x/\alpha, y/\beta) = (0.25, 0.25)$ with an instrumented hammer, and the acceleration was measured with a miniature accelerometer (1 g mass) at points $(x/\alpha, y/\beta) = (0.5, 0.5)$ and $(x/\alpha, y/\beta) = (0.25, 0.75)$. The signals from the hammer and the accelerometer were recorded with a high-speed digital data acquisition system and then processed using FFT software to obtain the frequency response functions of the plate. The accelerance of the plate at the previously mentioned points is shown in Fig. 4.

The predicted response was synthesized from the calculated modal damping and natural frequencies using a modal superposition technique (Fig. 4) with frequency effects included as described in the previous section. With the exception of the first mode, the predicted response sufficiently reproduces the measured one. The mismatch and higher damping of the first mode was also observed in the test of a monolithic aluminum plate and was thus attributed to imperfections in the experimental supports. There is some underestimation of the damping in the predicted response, which may be attributed to friction and air damping present in the experiment. However, both predicted and measured results fall within the range of uncertainty predicted from the upper and lower bounds of scatter in the manufacturer's data for this polymer film damping. The agreement is improved at higher modes, because the effects of the supports are less dominant compared to the shear damping contributions of the damping material.

Applications and Discussion

This section presents applications of the developed methodology on square laminated graphite/epoxy simply supported (SS) plates with interlaminar damping layers. The dimensions of the plate were assumed 11.8 in. × 11.8 in. (30 cm × 30 cm). The composite material was HM-S graphite/epoxy with elastic and damping properties given in Ref. 6. Unless otherwise stated, the FVR of the composite plies was 0.50. The shear modulus and shear loss factor of the interlaminar damping layer were 0.9 kpsi (6.2 MPa) and 1.02 respectively and represent average values of a typical commercial damping polymer (ScotchDamp ISD112, 3M Corp.)[18] at room temperature. Experimental data regarding the normal loss factor and Young's modulus of the damping polymer were not available. Because the present theory includes provisions for normal damping and modulus, a Poisson's ratio of 0.3 and a very low normal loss factor (0.016) were assumed for the damping polymer to ensure minimal contribution on the damping of the plate. This assumption was further reinforced by parametric studies that quantified the insensitivity of the modal characteristics (natural frequencies and damping) of the plate to the normal damping and the Poisson's ratio of the damping layer. The effects of frequency on the properties of the damping polymer were neglected here to isolate the effects of composite anisotropy and inhomogeneity on the performance of the damping layers. The nominal thickness t_i of the damping layer was equal to the typical thickness of a composite ply $t_l = 0.005$ in. (0.13 mm). In all cases a concentrated vertical load of 100 lb (445 N) was applied at the center of the plate. Linear interpolation functions $F^j(z)$ were used to calculate the in-plane displacements through the thickness of the laminate.

The ply-stacking sequence is represented using the traditional convention, but interlaminar damping layers of thickness t_i are identified with the symbol i. For comparison purposes, calculated results for aluminum plates are also presented. In order to maintain solidarity with the laminate notation, an aluminum layer of thickness equal to the thickness of k plies will be identified as Al_k. All laminate configurations were symmetric. The modal loss factor is normalized by the shear loss factor of the polymer and will be referred to as "normalized modal damping" in the following paragraphs.

Predicted modal damping, natural frequencies, and static deflections at the center of an aluminum $(Al_4/i/Al_4)_s$ and

Table 1 Static and dynamic characteristics of composite plates with interlaminar layers ($t_i = 0.005$ in.; numbers in parentheses indicate mode order)

	$(Al_4/i/Al_4)_s$	$(0_4/i/0_4)_s$	$(0_4/i/90_4)_s$	$(0_2/90_2/i/0_2/90_2)_s$
Areal density, 10^{-3} lb/in.^{2}	7.95	4.92	4.92	4.92
Static deflection (center), in.	0.334	0.604	0.496	0.456
Normalized modal damping				
Mode 1	0.131 (1, 1)	0.153 (1, 1)	0.153 (1, 1)	0.098 (1, 1)
Mode 2	0.259 (1, 2)	0.126 (1, 2)	0.066 (1, 2)	0.266 (1, 2)
Mode 3	0.259 (2, 1)	0.104 (1, 3)	0.433 (2, 1)	0.252 (2, 1)
Mode 4	0.346 (2, 2)	0.110 (1, 4)	0.355 (2, 2)	0.277 (2, 2)
Mode 5	0.374 (1, 3)	0.370 (2, 1)	0.033 (1, 3)	0.438 (1, 3)
Mode 6	0.374 (3, 1)	0.355 (2, 2)	0.218 (2, 3)	0.395 (2, 3)
Mode 7	0.415 (2, 3)	0.319 (2, 3)	0.598 (3, 1)	0.381 (3, 1)
Mode 8	0.415 (3, 2)	0.134 (1, 5)	0.553 (3, 2)	0.380 (2, 3)
Mode 9	0.448 (1, 4)	0.277 (2, 4)	0.028 (1, 4)	0.545 (1, 4)
Mode 10	0.448 (4, 1)	0.249 (2, 5)	0.438 (3, 3)	0.418 (3, 3)
Natural frequencies, Hz				
Mode 1	115.7	119.9	119.9	124.0
Mode 2	265.0	152.7	211.8	272.6
Mode 3	265.0	230.1	354.8	357.7
Mode 4	395.2	351.2	402.4	437.7
Mode 5	474.5	383.4	409.3	495.2
Mode 6	474.5	402.3	541.7	606.7
Mode 7	585.6	447.7	635.2	688.7
Mode 8	585.6	508.7	667.9	736.7
Mode 9	722.5	531.4	697.6	747.2
Mode 10	722.5	656.5	766.7	851.6

various graphite/epoxy damped plates, $(0_4/i/0_4)_s$, $(0_4/i/90_4)_s$, and $(0_2/90_2/i/0_2/90_2)_s$, are shown in Table 1. All plates have high modal damping values. The laminates with the higher anisotropy in the composite sublaminates, i.e., $(0_4/i/0_4)_s$ and $(0_4/i/90_4)_s$, exhibit the higher damping in the fundamental mode. The $(0_4/i/90_4)_s$ laminate exhibits the higher anisotropy variation through the thickness among all plates; this seems to have resulted in some higher modal damping values. Interestingly, this laminate has comparable static stiffness and natural frequency with the $(0_2/90_2/i/0_2/90_2)_s$ laminate, which illustrates the possibility for higher damping values in some modes without significantly penalizing other structural characteristics. The high damping of the unidirectional composite laminate was attributed in part to the lower stiffness of the plate. The composite plates have higher static deflections but lower areal density than the aluminum plate; as a result, they exhibit slightly higher fundamental frequencies. The damping of the higher modes varies widely and depends on the respective mode shape. The variation is more predominant for the composite plates.

The variations of the first modal damping, natural frequency, and static deflection at the center of the plate are plotted in Fig. 5 as functions of the damping layer thickness. The thickness of the composite sublaminates was kept constant, therefore, the total laminate thickness was varied. The layer thickness t_i is normalized by the nominal ply thickness $t_l = 0.005$ in. For layer thicknesses in the range of practical interest, the laminate with the higher anisotropy through the thickness $(0_4/i/90_4)_s$ provides consistently higher damping than the aluminum $(Al_4/i/Al_4)_s$ and $(0_2/90_2/i/0_2/90_2)_s$ laminates. These results are consistent with the expectation that composite laminates will induce higher interlaminar shear stresses in the interlaminar layer, in order to balance the elastic anisotropy and nonuniformity of adjacent plies, as opposed to traditional isotropic laminates, where interlaminar stresses will only balance the bending stresses through the thickness. For all laminates the modal damping increased with thickness

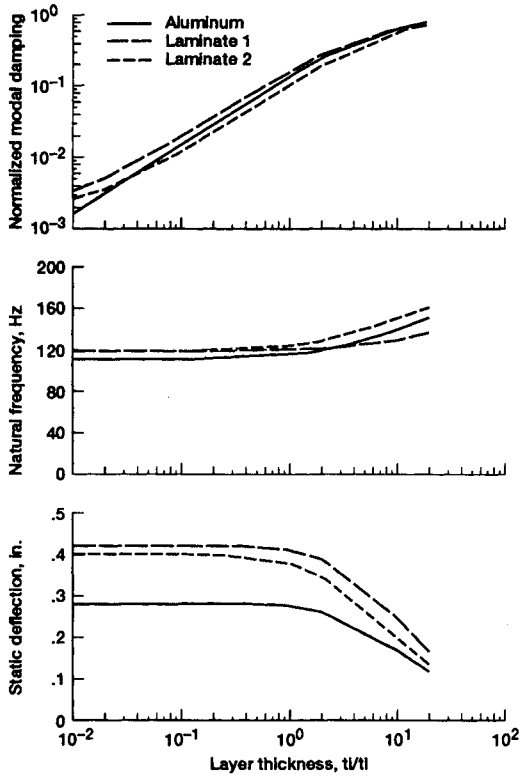

Fig. 5 Effect of damping layer thickness on static and dynamic characteristics of composite plates [aluminum = $(Al_4/i/Al_4)_s$; laminate 1 = $(0_4/i/90_4)_s$; laminate 2 = $(0_2/90_2/i/0_2/90_2)_s$].

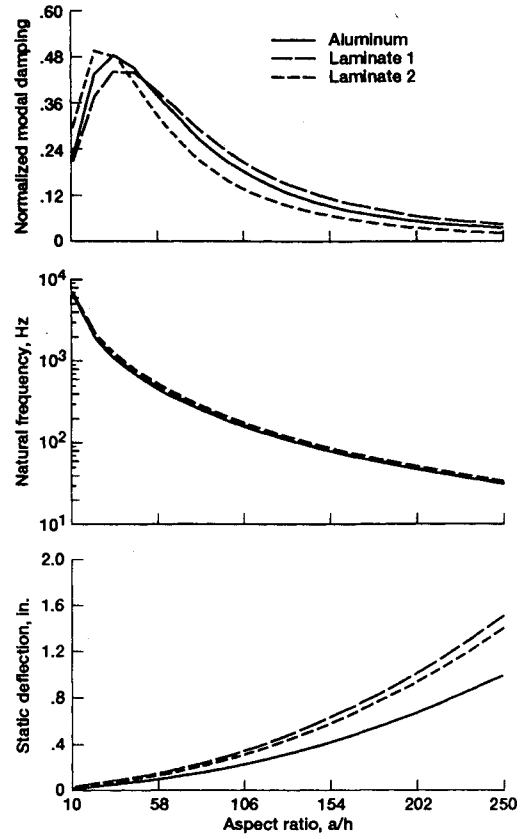

Fig. 6 Effect of plate aspect ratio on static and dynamic characteristics of composite plates [aluminum = $(Al_4/i/Al_4)_s$; laminate 1 = $(0_4/i/90_4)_s$; laminate 2 = $(0_2/90_2/i/0_2/90_2)_s$].

and tends to reach a maximum at higher thickness values. It was observed that, for plates of lower aspect ratio a/h, the peak in the modal damping shifts toward lower thicknesses. Finally, it seems that a critical damping layer thickness exists (in this case approximately equal to the ply thickness) such that damping layers with less or equal thickness will add low but significant damping, with negligible effects on the structural properties (static deflection, natural frequency).

Figure 6 shows the predicted variations of modal damping, natural frequency, and static deflection with the aspect ratio of the plate (a/h). As was expected, the modal damping of all plates increases at lower aspect ratios because shear prevails over flexure. Interestingly, the damping reaches a peak at very low aspect ratios and then decreases again. Intuitively, at very low aspect ratios through-the-thickness deformations will gradually prevail over shear and the effectiveness of the damping layer will be decreased. Nevertheless, the kinematic assumptions of the DLDT are not expected to be valid at the regime of very low aspect ratios because the present approach assumes negligible through-the-thickness strains. Both natural frequency and static stiffness consistently increase with lower aspect ratios.

Figure 7 presents the variation of modal damping, natural frequency, and static deflection as functions of the FVR of the inner and outer composite sublaminates with respect to the damping layers. This figure demonstrates one unique advantage of composite laminates (i.e., the additional tailoring capacity they can introduce). In both laminates the FVR variation of the outer sublaminate has a definite effect on the modal damping of the plate. The damping increases almost linearly with the FVR, indicating that the most important composite parameter is the longitudinal modulus. Since both natural frequency and static stiffness also increase with the FVR of the outer sublaminate, the obvious choice is to have outer sublaminates of very high FVR. The modal damping is

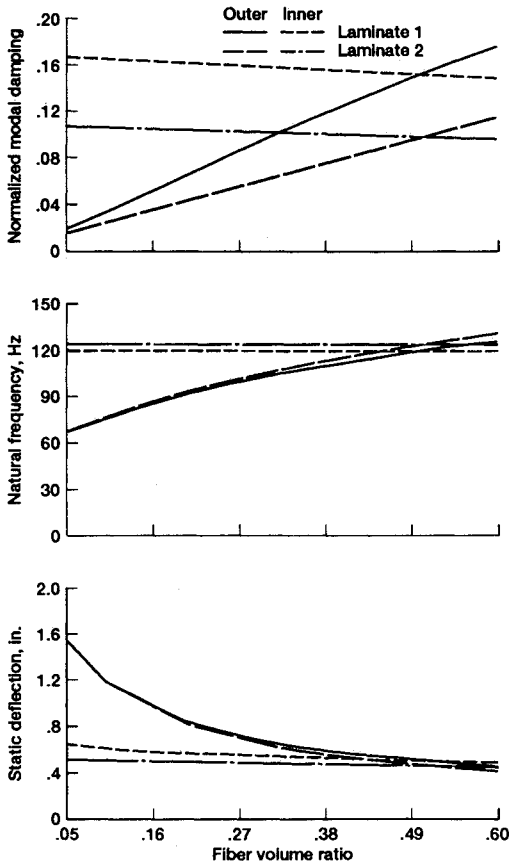

Fig. 7 Effect of fiber volume ratio on static and dynamic characteristics of composite plates [laminate 1 = $(0_4/i/90_4)_s$; laminate 2 = $(0_2/90_2/i/0_2/90_2)_s$].

less sensitive to FVR variations of the inner sublaminate and decreases slightly with FVR.

Summary

This paper presented recent research developments in integrated damping mechanics for composite laminates with interlaminar damping layers. Damping mechanics for such composite laminates and plates were developed based on a discrete-layer laminate theory. The discrete-layer displacement field of variable degrees of freedom allowed the calculation of the interlaminar shear strains in the damping layer and composite plies and the subsequent prediction of interlaminar shear damping. A semianalytical method was developed for the prediction of the damped dynamic characteristics of composite laminates with interlaminar damping layers.

Experimentally measured and predicted dynamic responses of a graphite/epoxy composite plate with co-cured damping layers were compared to illustrate the accuracy of the method. More applications on graphite/epoxy orthotropic (unidirectional or cross ply) composite plates with layers of damping polymers demonstrated that composite laminates have dynamic characteristics comparable to those of geometrically identical aluminum plates. In addition, composite plates with strong anisotropy variations between the restraining sublaminates exhibited potential for higher damping than geometrically equivalent aluminum plates. The effects of thickness aspect ratio, damping layer thickness, and composite fiber volume ratio on the modal damping, natural frequency, and static deflection were investigated. Overall, the results have demonstrated the potential of embedded interlaminar damping layers in composite laminates. Moreover, they demonstrated the merits of the developed damping mechanics. Future studies will address the effects of damping layers on the laminate strength, bucking, and impact resistance.

Appendix

Off-axis ply stiffness matrix $[E_c]$ (Ref. 14):

$$\{\sigma_c\} = [E_c]\{e_c\} \tag{A1}$$

Transformation matrices:

$$[R] = \begin{bmatrix} m^2 & n^2 & 0 & 0 & 0 & 2mn \\ n^2 & m^2 & 0 & 0 & 0 & -2mn \\ 0 & 0 & 1 & 0 & 0 & 0 \\ 0 & 0 & 0 & m & -n & 0 \\ 0 & 0 & 0 & +n & m & 0 \\ -mn & mn & 0 & 0 & 0 & m^2 - n^2 \end{bmatrix}$$

$$m = \cos\theta, \qquad n = \sin\theta \tag{A2}$$

$$[R]^{-1} = [R(-\theta)] \tag{A3}$$

On-axis damping matrix:

$$[\eta_l] = \begin{bmatrix} \eta_{l1} & 0 & 0 & 0 & 0 & 0 \\ 0 & \eta_{l2} & 0 & 0 & 0 & 0 \\ 0 & 0 & \eta_{l3} & 0 & 0 & 0 \\ 0 & 0 & 0 & \eta_{l4} & 0 & 0 \\ 0 & 0 & 0 & 0 & \eta_{l5} & 0 \\ 0 & 0 & 0 & 0 & 0 & \eta_{l6} \end{bmatrix} \tag{A4}$$

The off-axis ply damping matrix is nondiagonal and has the following general form:

$$[\eta_c] = \begin{bmatrix} \eta_{c11} & \eta_{c12} & 0 & 0 & 0 & \eta_{c16} \\ \eta_{c21} & \eta_{c22} & 0 & 0 & 0 & \eta_{c26} \\ 0 & 0 & \eta_{c33} & 0 & 0 & 0 \\ 0 & 0 & 0 & \eta_{c44} & \eta_{c45} & 0 \\ 0 & 0 & 0 & \eta_{c54} & \eta_{c55} & 0 \\ \eta_{c61} & \eta_{c62} & 0 & 0 & 0 & \eta_{c66} \end{bmatrix} \tag{A5}$$

Acknowledgment

The authors acknowledge the contributions of Christos C. Chamis for his valuable comments, Peter Addente for fabricating the composite plates, and 3M Corporation for providing samples of the damping polymer.

References

[1]Torvik, P. J., "The Analysis and Design of Constrained Layer Damping Treatments," *Damping Applications for Vibration Control,* edited by P. Torvik, American Society of Mechanical Engineers, New York, 1980, pp. 27–51.

[2]Schultz, A. B., and Tsai, S. W., "Measurements of Complex Dynamic Moduli for Laminated Fiber-Reinforced Composites," *Journal of Composite Materials,* Vol. 3, July 1969, pp. 434–443.

[3]Adams, R. D., and Bacon, D. G. C., "Effect of Fibre Orientation and Laminate Geometry on the Dynamic Properties of CFRP," *Journal of Composite Materials,* Vol. 7, Oct. 1973, pp. 402–428.

[4]Saravanos, D. A., and Chamis, C. C., "Mechanics of Damping for Fiber Composite Laminates Including Hygro-Thermal Effects," *AIAA Journal,* Vol. 28, No. 10, 1990, pp. 1813–1819.

[5]Siu, C. C., and Bert, C. W., "Sinusoidal Response of Composite-Material Plates with Material Damping," *ASME Journal of Engineering for Industry,* Vol. 96, No. 2, May 1974, pp. 603–610.

[6]Saravanos, D. A., and Chamis, C. C., "Computational Simulation of Damping in Composite Structures," *Journal of Reinforced Plastics and Composites,* Vol. 10, No. 3, May 1991, pp. 256–277; also NASA TM-102567, 1990.

[7]Saravanos, D. A., and Chamis, C. C., "A Computational Methodology for Optimizing the Passive Damping of Composite Structures," *Journal of Polymer Composites,* Vol. 11, No. 6, 1990, pp. 328–336.

[8]Chen, G. S., and Wada, B. K., "Passive Damping for Space Truss Structures," *Proceedings of the AIAA/ASME/ASCE/AHS 29th Structures, Structural Dynamics and Materials Conference,* Washington, DC, 1988, pp. 1742–1749.

[9]Bronowicki, A. J., and Diaz, H. P., "Analysis, Optimization, Fabrication and Test of Composite Shells with Embedded Viscoelastic Layers," *Proceedings of Damping '89,* Wright-Patterson AFB, OH, WRDC-TR-89-3116-Vol.-1, Sec. HC, Paper HCB, 1989.

[10]Barrett, D. J., "A Design for Improving the Structural Damping Properties of Axial Members," *Proceedings of Damping '89,* Wright-Patterson AFB, OH, WRDC-TR-89-3116-Vol.-1, Sec. HC, Paper HCB, 1989.

[11]Barrett, D. J., "An Anisotropic Laminated Damped Plate Theory," Naval Air Development Center, Rept. NADC-90066-60, Warminster, PA, July 1990.

[12]Mantena, R. P., Gibson, R. F., and Shwilong, H. J., "Optimal Constrained Viscoelastic Tape Lengths for Maximizing Damping in Laminated Composites," *Proceedings of Damping '89,* Wright-Patterson AFB, OH, WRDC-TR-89-3116-Vol.-1, Sec. IA, Paper IAB, 1989.

[13]Rao, V. S., Sun, C. T., and Sankar, B. V., "Damping and Vibration Control of Some Laminated Composite Beams Using Add-On Viscoelastic Materials," *Proceedings of Damping '89,* Wright-Patterson AFB, OH, WRDC-TR-89-3116-Vol.-2, Sec. VA, Paper VAA, 1989.

[14]Murthy, P. L. N., and Chamis, C. C., "ICAN: Integrated Composite Analyzer," AIAA Paper 84-0974, May 1984.

[15]Saravanos, D. A., and Chamis, C. C., "Unified Micromechanics of Damping for Unidirectional Fiber Composites," *Journal of Composites Technology and Research,* Vol. 12, No. 1, 1990, pp. 31–40.

[16]Noor, A. K., and Burton, S. W., "Assessment of Computational Models for Multilayer Composite Shells," *Applied Mechanics Reviews,* Vol. 43, No. 4, 1990, pp. 67–96.

[17]Barbero, E. J., Reddy, J. N., and Teply, J., "An Accurate Determination of Stresses in Thick Composite Laminates Using a Generalized Plate Theory," *International Journal for Numerical Methods in Engineering,* Vol. 29, Jan. 1990, pp. 1–14.

[18]Drake, M. L., "Damping Properties of Various Materials," Research Lab., Univ. of Dayton, AFWAL-TR-88-4248, Dayton, OH, March 1989.